



# The University of Bradford Institutional Repository

<http://bradscholars.brad.ac.uk>

This work is made available online in accordance with publisher policies. Please refer to the repository record for this item and our Policy Document available from the repository home page for further information.

To see the final version of this work please visit the publisher's website. Available access to the published online version may require a subscription.

Link to original published version: [http://dx.doi.org/10.1061/\(ASCE\)ST.1943-541X.0000351](http://dx.doi.org/10.1061/(ASCE)ST.1943-541X.0000351)

Citation: Yang KH and Ashour AF (2011) Strut-and-tie model based on crack band theory for deep beams. *Journal of Structural Engineering*, 137(10): 1030-1038.

Copyright statement: © 2011 ASCE. Reproduced in accordance with the publisher's self-archiving policy.



# STRUT-AND-TIE MODEL BASED ON CRACK BAND THEORY FOR DEEP BEAMS

Keun-Hyeok Yang<sup>a</sup> and Ashraf F. Ashour<sup>b</sup>

<sup>a</sup> *Corresponding author, Department of Architectural Engineering, Mokpo National University, Mokpo, Jeonnam, South Korea, Tel: +82 (0)61 450 2456, Fax: +82 (0)61 450 6454, E-mail: [yangkh@mokpo.ac.kr](mailto:yangkh@mokpo.ac.kr)*

<sup>b</sup> *EDT1, School of Engineering, Design and Technology, University of Bradford, Bradford, BD7 1DP, U.K.*

**Biography:** **K. H. Yang** is an assistant professor at Mokpo National University, South Korea. He received his MSc and PhD degrees from Chungang University, South Korea. He was a visiting research fellow at the University of Bradford, UK. His research interests include recycling strengthening, plasticity and shear of reinforced eco-friendly concrete structures.

**A. F. Ashour** is a senior lecturer at the University of Bradford, UK. He obtained his BSc and MSc degrees from Mansoura University, Egypt and his PhD degree from Cambridge University, UK. His research interests include shear, plasticity, strengthening and optimisation of reinforced concrete and masonry structures.

## ABSTRACT

A simplified strut-and-tie model including size effect based on the crack band theory of fracture mechanics is proposed to evaluate the shear capacity of deep beams. Concrete struts are idealised as uniformly tapered prismatic members having a stress relief strip, whereas horizontal and vertical

shear reinforcement is assumed to be an internally statically indeterminate system. The shear transfer mechanism of concrete and shear reinforcement is then driven using the energy equilibrium in the stress relief strip and crack band zone of concrete struts. The unknown coefficients of the proposed model are determined by regression analysis of an extensive database including 637 simple deep beam specimens failed in shear. The shear capacity predictions of deep beams obtained from the present models are in better agreement with test results than those determined from strut-and-tie models proposed by ACI 318-05, EC 2, and Tan and Cheng. The mean, standard deviation, and coefficient of variation of the ratio between predicted using the present model and measured shear capacities of deep beams are 1.002, 0.250 and 0.250, respectively. In addition, the trend of the shear capacity of deep beams against different parameters as predicted by the present models has a consistent agreement with that observed from experimental results. In particular, the present model shows the normalized shear capacity of deep beams is proportional to  $(h)^{-0.25}$ , where  $h$  is the section overall depth.

**Keywords:** size effect, deep beams, shear capacity, strut-and-tie model, fracture mechanics.

## INTRODUCTION

Reinforced concrete deep beams are commonly classified as a discontinuity region (D-region), where the strain distribution over their cross-section depth is nonlinear, even in the elastic stage.<sup>1</sup> In addition, extraordinarily high concentric top loads applied to deep beams are directly transferred to supports through concrete struts. As a result, the increase of shear capacity according to the decrease of shear span-to-depth ratio is more significant in deep beams than slender beams. It has been also pointed out<sup>2,3</sup> that the empirical shear provisions of ACI 318-99<sup>4</sup> based on diagonal cracking shear strength of slender beams fail to provide a rational approach to explain the shear transfer

mechanisms of concrete web and shear reinforcement, which lead to unconservative shear design of deep beams.

Strut-and-tie models (STM) have been generally recognized as a good design tool for D-region members including deep beams.<sup>5-8</sup> In addition, most current design codes<sup>3, 9, 10</sup> have recommended the STM approach as a design tool for deep beams. However, shear capacity of deep beams evaluated from STMs is strongly dependent on the effectiveness factor of concrete.<sup>11</sup> Foster and Malik<sup>12</sup> evaluated different effectiveness factor formulae used in STMs of nonflexural members such as deep beams, corbels and nibs. They concluded that effectiveness factor models based primarily on concrete strength are found to have poor correlation with test results of 135 nonflexural structural elements. In addition, most of STMs proposed for deep beams disregard the size effect. Tan and Cheng<sup>13</sup> also showed that size effect has to be considered in the effective strength of concrete struts to reasonably evaluate the shear capacity of deep beams with large sections.

Horizontal and vertical shear reinforcements in deep beams are provided to control the diagonal crack width and enhance the shear capacity and ductility of concrete struts.<sup>2, 3</sup> Although most codes of practice<sup>3, 9</sup> recommend the use of a minimum amount of shear reinforcement in two orthogonal directions in each face for bottle-shape strut, no specific guidelines on the shear transfer mechanism of shear reinforcement are provided.

The present study proposes a size effect based STM to predict shear capacity of deep beams. The shear transfer capacities of concrete struts and reinforcing steel bars are modelled following the concept of the crack band theory<sup>15</sup> of fracture mechanics. The basic formulas identifying the shear transfer mechanism of concrete and shear reinforcement are driven using the energy equilibrium in the stress relief strip and crack band zone of concrete struts. An extensive database for deep beams established by Yang et al.<sup>16, 17</sup> is used to determine the experimental constants and unknown coefficients in the proposed STM. Statistical distributions of predictions obtained from the proposed STM are compared with those determined from STMs recommended by ACI 318-05<sup>3</sup>, EC 2<sup>9</sup> and

Tan and Cheng<sup>13</sup>. In addition, a parametric study is carried out to verify whether the critical variables are suitably modelled in the STM.

## **RESEARCH SIGNIFICANCE**

Although the size effect in deep beams is more prominent than slender beams, it is commonly disregarded in most of the existing STMs. In addition, few, if any, specific guideline on the shear transfer capacity of horizontal and vertical shear reinforcements by truss action is available in the literature. The crack band theory-based STM proposed in the present study identifies the shear transfer mechanisms of concrete struts and reinforcing bars considering size effect. This study also examines the applicability of STMs recommended by ACI 318-05<sup>3</sup>, EC 2<sup>9</sup>, and Tan and Cheng<sup>13</sup> using an extensive database of deep beams.

## **STRUT-AND-TIE MODEL FOR SIMPLY SUPPORTED DEEP BEAMS**

Main shear transfer systems in STMs are struts representing compression stress fields in concrete and tie action of longitudinal reinforcement having one or several layers. Concrete struts in deep beams commonly considered as bottle-shaped struts, which can be idealized schematically as prismatic or uniformly tapered members within shear spans.<sup>3, 7</sup> Axial forces in struts and ties intersect at nodes. Applied forces are transferred from the inclined struts to other struts, to ties and to reactions through nodal zones representing concrete around a node. Therefore, the schematic STM for simple deep beams can be generally idealized as shown in Fig. 1.

## **Crack band theory background**

In the crack band model proposed by Bažant<sup>18</sup>, a crack is simulated by a fracture band of a fixed thickness, which is idealized as a continuum having a uniform strain distribution across the band. It

is also considered that fracture of concrete is caused by a crack band formed from a number of micro-cracks rather than a single line crack. A stress-strain relation with softening is associated with a certain width of the crack band, which represents a reference width and is related to a material property. To simply apply the crack band model to concrete members failed in high brittleness such as shear fracture, the prepeak region of stress-strain relation of concrete is generally regarded as a linear equation, and postpeak region of that is neglected as the area of postpeak region at failure, representing the extra energy supply required to break a unit volume of material in the crack band, is very small.

### **Basic assumption**

Modes of deep beam failure are generally classified into four groups: compressive failure of concrete struts, yielding or anchorage failure of longitudinal reinforcement ties, and bearing failure of nodal zones. Among these modes of failure, compressive failure of concrete struts is the most common<sup>1</sup> and accordingly it is only considered here. The following assumptions are made in the developed STM:

- Stress relief strips in concrete struts concentrate along diagonal cracks as shown in Fig. 2.
- Crack band with a number of axial splitting micro-cracks progresses to a certain limit, which eventually leads to failure of deep beams.
- Reinforcing bars are perfectly bonded to concrete and their dowel action is ignored.
- Stresses in reinforcing bars at beam failure are less than their own yield strength. In general, longitudinal reinforcement keeps within the elastic state when the structural failure of deep beams are governed by compressive crushing of concrete struts.<sup>19</sup> In addition, many investigations<sup>2, 11, 16</sup> showed that vertical and horizontal shear reinforcements do not commonly reach the yield strength when shear span-to-overall depth ratio is less than approximately 1.0 and more than 1.0, respectively.

▪ Shear capacity,  $V_n$ , of deep beams is the sum of shear transfer capacity of concrete and longitudinal reinforcement,  $V_c$ , and shear transfer capacity of shear reinforcement,  $V_s$ , as below:

$$V_n = V_c + V_s \quad (1)$$

### Shear transfer capacity by strut-and-tie action

According to fracture mechanics, the propagation of crack band dissipates the strain energy stored in concrete struts and longitudinal reinforcement. Therefore, the loss of strain energy,  $\Delta U_c$ , in a deep beam without shear reinforcement due to stress relief during the formation of the crack band can be approximately obtained from elastic theory as<sup>15</sup>:

$$\Delta U_c = -\frac{\sigma_N^2}{2E_c} b_w w_f jd / \sin \theta - \frac{\sigma_s^2}{2E_s} w_f A_s \sin \theta \quad (2)$$

where  $b_w$  = width of beam section,  $w_f$  = width of stress relief strip,  $jd$  = depth between top and bottom nodes,  $\theta$  = angle between concrete struts and longitudinal axis,  $E_c$  and  $E_s$  = moduli of elasticity of concrete and reinforcing steel bars, respectively, and  $A_s$  = area of longitudinal reinforcement. It should be noted that the minus sign in Eq. (2) indicates an energy loss. Axial stresses in concrete strut,  $\sigma_N$ , and longitudinal reinforcement,  $\sigma_s$ , of simple deep beams can be expressed in the following form:

$$\sigma_N = \frac{V / \sin \theta}{b_w w_s} \quad (3)$$

$$\sigma_s = \frac{V / \tan \theta}{A_s} \quad (4)$$

where  $V$  = external shear force applied to deep beams, and  $w_s$  = width of concrete strut. The loss of strain energy of concrete struts and longitudinal reinforcement is dependent on  $w_f$  as given in Eq. (2). Hence, the energy release rate,  $\mathfrak{S}$ , per unit width of beam due to the growth of the crack band at the stress relief strip is obtained from the basic theory of fracture mechanics<sup>15</sup> as below:

$$\mathfrak{S} = -\frac{1}{b_w} \left[ \frac{\partial(\Delta U_c)}{\partial w_f} \right] = \frac{V^2 jd}{2E_c b_w^2 w_s^2 \sin^3 \theta} + \frac{V^2 \sin \theta}{2nE_c b_w A_s \tan^2 \theta} \quad (5)$$

where  $n = E_s / E_c =$  modular ratio. The number of axial splitting micro-cracks in a crack band can be expressed as  $w_f / s_c$ , where  $s_c =$  average spacing of micro-cracks. Hence, the total energy  $W$  dissipated in the crack band is obtained from:

$$W = \frac{w_f}{s_c} b_w h_f G_f \quad (6)$$

where  $h_f =$  length of the crack band (see Fig. 2) and  $G_f =$  fracture energy of concrete. Differentiating  $W$  with respect to  $w_f$ , the energy,  $\mathfrak{R}$ , dissipated in the crack band per unit length of the band and unit width of the beam can be expressed by the following form<sup>15</sup>:

$$\mathfrak{R} = \frac{1}{b_w} \frac{\partial W}{\partial w_f} = \frac{h_f}{s_c} G_f \quad (7)$$

The energy dissipated,  $\mathfrak{R}$ , in Eq. (7) above indicates a crack growth resistance. From the energy equilibrium,  $\mathfrak{S} = \mathfrak{R}$ , the shear stress,  $v$ , of deep beams without shear reinforcement required for the propagation of the crack band can be derived as follows:

$$v = \frac{V}{b_w h} = \sqrt{2E_c G_f} \left( \frac{jd}{w_s^2 \sin^3 \theta} + \frac{\sin \theta}{n\rho_s d \tan^2 \theta} \right)^{-0.5} \frac{1}{h} \left( \frac{h_f}{s_c} \right)^{0.5} \quad (8)$$

where  $\rho_s = \frac{A_s}{b_w d} =$  longitudinal reinforcement ratio, and  $h$  and  $d =$  overall depth and effective depth of deep beam section, respectively. Bažant and Planas<sup>15</sup> showed that the crack band length  $h_f$  at the beam failure can be represented by the following relation:

$$h_f = \frac{w_f}{w_0 + w_f} h_0 \quad (9)$$



where  $h_0$  = a certain characteristic value representing the final length of the crack band, and  $w_0$  = a positive constant. Substituting Eq. (9) into Eq. (8), the ultimate shear stress,  $v_c$ , of deep beams without shear reinforcement due to compressive failure of concrete strut can be expressed as below:

$$v_c = \frac{V_c}{b_w h} = \sqrt{2E_c G_f} \left( \frac{jd}{w_s^2 \sin^3 \theta} + \frac{\sin \theta}{n\rho_s d \tan^2 \theta} \right)^{-0.5} \frac{1}{h} \left( \frac{h_0}{s_c} \right)^{0.5} \left( \frac{w_f}{w_0 + w_f} \right)^{0.5} \quad (10)$$

### Shear transfer contribution of shear reinforcement

One of several benefits of shear reinforcement in deep beams is that cracks are forced to redistribute at a closer spacing and over a wider area in concrete struts. Stresses in concrete struts are consequently redistributed and the width of concrete crushing zone spreads transversely (see Fig. 3). Considering the idealized crack band extension, the loss of strain energy,  $\Delta U_s$ , in vertical and horizontal shear reinforcements is expressed as follows:

$$\Delta U_s = -\frac{\sigma_{sv}^2}{2E_s} (w_f + w_i) A_{v1} \frac{jd \cos \theta}{s_v \tan \theta} - \frac{\sigma_{sh}^2}{2E_s} (w_f + w_i) A_{h1} \frac{jd \sin \theta}{s_h} \quad (11)$$

where  $s_v$  and  $A_{v1}$  = spacing and area, respectively, of vertical shear reinforcement,  $s_h$  and  $A_{h1}$  = spacing and area, respectively, of horizontal shear reinforcement, and  $w_i$  = width of crack band extension zone as shown in Fig. 3. In Eq. (11), the average stresses of vertical,  $\sigma_{sv}$ , and horizontal,  $\sigma_{sh}$ , shear reinforcements can be calculated as follows:

$$\sigma_{sv} = \frac{\alpha_v V_s s_v \tan \theta}{A_{v1} jd} \quad (12)$$

$$\sigma_{sh} = \frac{\alpha_h V_s s_h}{A_{h1} jd} \quad (13)$$

where  $V_s$  = shear transfer capacity of shear reinforcement, and  $\alpha_v$  and  $\alpha_h$  = proportions of shear force carried by vertical and horizontal shear reinforcements, respectively. Therefore, the energy

release rate  $\mathfrak{V}_s$  of shear reinforcement due to the extension of the crack band can be estimated by the following equation:

$$\mathfrak{V}_s = -\frac{1}{b_w} \left[ \frac{\partial(\Delta U_s)}{\partial w_i} \right] = \frac{V_s^2 \sin \theta}{2njdE_c} \left( \frac{\alpha_v^2}{\rho_v} + \frac{\alpha_h^2}{\rho_h} \right) \quad (14)$$

where  $\rho_v = A_{v1}/b_w s_v$  and  $\rho_h = A_{h1}/b_w s_h$  = ratios of vertical and horizontal shear reinforcements, respectively. As the total energy dissipated in the crack band extension zone due to shear reinforcement is  $W_s = \frac{w_i}{s_{ce}} b_w h_0 G_f$ , the crack growth resistance,  $\mathfrak{R}_s$ , of the crack band extension zone is obtained from<sup>15</sup>:

$$\mathfrak{R}_s = \frac{1}{b_w} \frac{\partial W_s}{\partial w_i} = \frac{h_0}{s_{ce}} G_f \quad (15)$$

where  $s_{ce}$  = spacing of axial splitting micro-cracks of the crack band extension zone of beams with shear reinforcement. Equating the loss of strain energy to crack growth resistance of crack band extension zone,  $\mathfrak{V}_s = \mathfrak{R}_s$ , shear stress,  $v_s$ , transferred by shear reinforcement is expressed as follows:

$$v_s = \frac{V_s}{b_w h} = \sqrt{\frac{2nE_c G_f jd}{h^2 \sin \theta} \left( \frac{\alpha_v^2}{\rho_v} + \frac{\alpha_h^2}{\rho_h} \right)^{-0.5} \left( \frac{h_o}{s_{ce}} \right)^{0.5}} \quad (16)$$

### Geometrical dimension of concrete struts

Considering the hydrostatic state of stress at nodal zones, the average width,  $w_s$ , at mid-depth of concrete struts can be calculated from the following equation:<sup>3, 20</sup>

$$w_s = \frac{1.8w_t \cos \theta + [(l_p)_E + (l_p)_P] \sin \theta}{2} \quad (17)$$

where  $w_t$  = height of bottom nodal zone,  $(l_p)_P$ , and  $(l_p)_E$  = widths of loading, and support plates, respectively, as shown in Fig. 1. ACI 318-05 pointed out that concrete struts of inclination less than

25 degrees are not effective in transferring applied external loads to supports. Therefore, the angle,  $\theta$ , of concrete struts presented in Fig. 1 can be obtained from:

$$\theta = \tan^{-1} \frac{jd}{a} \geq 25^\circ \quad (18)$$

The depth of the top node can be determined from the equilibrium of forces of the limit of resultant compressive force in the top node and the limit of resultant tensile force in the bottom node.<sup>2</sup> As the height of the top nodal zone is assumed to be  $0.8 w_t$  from the concrete effective stresses in the nodal zones, the distance between top and bottom nodes is calculated from the following equation:

$$jd = h - 0.9w_t \quad (19)$$

### Concrete properties

The modulus of elasticity of concrete is obtained from the equation specified in ACI 318-05<sup>3</sup>.

$$E_c = 4700\sqrt{f'_c} \text{ (in MPa)} \quad (20)$$

where  $f'_c$  = concrete compressive strength in MPa. Available literature on fracture energy of concrete is very scarce. The concrete fracture energy equations specified in CEB-FIP<sup>10</sup> is adopted in the present study as below:

$$G_f = G_{fo} \left( f'_c / f_{co} \right)^{0.7} \text{ for } f'_c \leq 80 \text{ MPa (11.6 ksi)} \quad (21 \text{ a})$$

$$G_f = 4.3G_{fo} \text{ for } f'_c > 80 \text{ MPa (11.6 ksi)} \quad (21 \text{ b})$$

where  $f_{co} = 10 \text{ MPa (1.45 ksi)}$  = reference concrete strength, and  $G_{fo}$  = basic fracture energy. CEB-FIP proposes different values of  $G_{fo}$  based on the maximum aggregate size,  $d_a$  (in mm), of concrete.

### Shear resistance of horizontal and vertical shear reinforcement

Fig. 4 shows shear transfer mechanisms for different shear reinforcement arrangements by truss action. The model with either vertical or horizontal shear reinforcement is a statically determinate

truss system. On the other hand, the idealized model with both horizontal and vertical shear reinforcements belongs to a statically internally indeterminate system as shown in Fig. 4 (c). Matamoros and Wong<sup>14</sup> concluded that average shear force carried by vertical and horizontal shear reinforcements can be reasonably evaluated using the stiffness method based on the assumption that the axial stiffnesses of all members are the same. Fig. 5 shows that the proportions of shear force carried by vertical and horizontal shear reinforcement against  $a/jd$  using the stiffness method. Based on the regression analysis of Fig. 5, the proportion of shear resistance of vertical and horizontal shear reinforcement can be calculated from:

$$\alpha_v = 1.0 \quad \text{for } \rho_h = 0 \text{ and } \rho_v > 0 \quad (22 \text{ a})$$

$$\alpha_v = 0.15(a/jd)^3 - 0.7(a/jd)^2 + (a/jd) \quad \text{for } \rho_h > 0 \text{ and } \rho_v > 0 \quad (22 \text{ b})$$

$$\alpha_h = a/jd \quad \text{for } \rho_v = 0 \text{ and } \rho_h > 0 \quad (23 \text{ a})$$

$$\alpha_h = -0.12(a/jd)^2 + 0.6(a/jd) \quad \text{for } \rho_v > 0 \text{ and } \rho_h > 0 \quad (23 \text{ b})$$

where  $\alpha_v$  and  $\alpha_h$  = proportions of shear force carried by vertical and horizontal shear reinforcements, respectively.

## STATISTICAL ANALYSIS OF TEST DATA

### Experimental database

The experimental database established by Yang et al.<sup>16, 17</sup> is used to evaluate and calibrate the proposed model. The frequency distribution of different parameters in the database is presented in Fig. 6. A total of 637 simple deep beam specimens failed in shear is collected from different sources. The frequency distribution of different parameters in the database is presented in Fig. 6. Some test specimens had no shear reinforcement whereas others were reinforced with vertical and horizontal shear reinforcement: the number of beam specimens in the database is 251 for beams without shear reinforcement, 165 for beams with only vertical shear reinforcement, 59 for beams with only

horizontal shear reinforcement, and 162 for beams with orthogonal shear reinforcement. The shear span-to-overall depth ratio  $a/h$  in the database ranged from 0.23 to 2.0. The beam specimens were made of concrete having a very low  $f'_c$  as 11 MPa (1.595 ksi) and a high  $f'_c$  of 120 MPa (17.4 ksi). The section overall depth,  $h$ , of most of the specimens varied between 300 mm (11.7 in.) and 700 mm (27.3 in.), though some specimens have a small depth below 300 mm (11.7 in.) and a few specimens have a relatively large depth above 1000 mm (39 in.).

## Model calibration

### Deep beams without shear reinforcement

Bažant and Planas<sup>15</sup> showed that  $(h_0/s_c)$  in Eq. (10) is an experimental constant, independent on  $h$  and  $w_f/h$ , and  $w_o/h$  can be also assumed as constant parameters. Hence,  $w_f/(w_o + w_f)$  in Eq. (10) can be regarded as a function of the section overall depth,  $h$ , normalized by the maximum aggregate size,  $d_a$ , for dimensional purposes. The normalized shear capacity,  $v_c/v_{pc}$ , of deep beam specimens without shear reinforcement extracted from the database is plotted against  $h/d_a$  in Fig. 7,

$$\text{where } v_{pc} = \sqrt{2E_c G_f} \left( \frac{jd}{w_s^2 \sin^3 \theta} + \frac{\sin \theta}{n\rho_s d \tan^2 \theta} \right)^{-0.5} \frac{1}{h}.$$

The best fit curve of the experimental results presented in Fig. 7 concludes that the optimum values of  $(h_0/s_c)^{0.5}$  and  $[w_f/(w_o + w_f)]^{0.5}$  can be assumed as 0.65 and  $(h/d_a)^{0.75}$ , respectively. As a result, shear transfer capacity of deep beams without shear reinforcement can be predicted from:

$$v_c = \frac{V_c}{b_w h} = 0.919 \sqrt{E_c G_f} \left( \frac{jd}{w_s^2 \sin^3 \theta} + \frac{\sin \theta}{n\rho_s d \tan^2 \theta} \right)^{-0.5} \frac{1}{h} \left( \frac{h}{d_a} \right)^{0.75} \quad (24)$$

Equation (24) clearly shows that shear stress capacity of deep beams without shear reinforcement is proportional to  $(h)^{-0.25}$ .

### Contribution of shear reinforcement

The crack distribution in concrete struts is commonly dependent on shear reinforcement as observed in test results<sup>21</sup>, therefore  $h_o / s_{ce}$  in Eq. (16) should be a function of the amount and configuration of shear reinforcement. It was also shown that the effectiveness of horizontal shear reinforcement increases with the decrease of  $a / jd$ , whereas that of vertical shear reinforcement increases with the increase of  $a / jd$ .<sup>2, 21</sup> However, the proportion of shear force transferred by shear reinforcement increases with the increase of  $a / jd$  as predicted from the elastic truss analysis and plotted in Fig. 5. Therefore, in order to improve the regression analysis for shear reinforcement and to avoid over fitting, the shear reinforcement ratio is normalised by  $\rho_0$  as pointed out by Bažant, and Sun<sup>22</sup>, where

$$\frac{1}{\rho_0} = 0.5 \left[ 1 + \tanh \left\{ \left( 2 \frac{a}{jd} - 2 \right) (2 \sin \beta - 1) \right\} \right] \quad (25)$$

and  $\beta =$  angle of shear reinforcement to the longitudinal axis of deep beams. For horizontal shear reinforcement ( $\beta = 0$ ), the coefficient  $1 / \rho_{ho}$  smoothly changes from 1.0 to 0.0, whereas, for vertical shear reinforcement ( $\beta = 90^\circ$ ),  $1 / \rho_{vo}$  smoothly increases from 0.0 to a finite value of 1.0, as  $a / jd$  increases from 0 to 2.0.

Normalized shear stress,  $v_s / v_{ps}$ , of shear reinforcement obtained from the database is plotted against the amount and configuration of shear reinforcement in Fig. 8, where

$$v_{ps} = \sqrt{\frac{2nE_c G_f jd}{h^2 \sin \theta} \left( \frac{\alpha_v^2}{\rho_v} + \frac{\alpha_h^2}{\rho_h} \right)^{-0.5}}. \text{ In Fig. 8, the shear transfer capacity of shear reinforcement, } V_s,$$

is obtained from the difference of the shear capacity of deep beam with shear reinforcement and that of the corresponding deep beam without shear reinforcement,  $(V_n)_{w/o}$ .<sup>2</sup> Regression analysis of test

results in fig. 8 suggests that  $(h_o / s_{ce})^{0.5}$  can be assumed as  $1.75 \left( \frac{100\rho_v}{\rho_{v0}} + \frac{100\rho_h}{\rho_{h0}} \right)^{0.375}$ , though the

scatter of the test data is relatively large. As a result, shear transfer capacity carried by shear reinforcement due to truss action can be proposed as follows:

$$v_s = \frac{V_s}{b_w h} = 2.47 \sqrt{\frac{nE_c G_f j d}{h^2 \sin \theta} \left( \frac{\alpha_v^2}{\rho_v} + \frac{\alpha_h^2}{\rho_h} \right)^{-0.5} \left( \frac{100\rho_v}{\rho_{vo}} + \frac{100\rho_h}{\rho_{ho}} \right)^{0.375}} \quad (26)$$

## COMPARISONS WITH TEST RESULTS

Table 1 gives the mean,  $\gamma_{cs,m}$ , standard deviation,  $\gamma_{cs,s}$ , and coefficient of variation,  $\gamma_{cs,v}$ , of the ratio between predicted and measured shear capacities,  $\gamma_{cs} = (V_n)_{Pre.} / (V_n)_{Exp.}$ , of deep beams in the database obtained from STMs proposed by ACI 318-05<sup>3</sup>, EC 2<sup>9</sup>, Tan and Cheng<sup>13</sup> and the current approach. The distributions of  $\gamma_{cs}$  for total specimens in the database against the section overall depth,  $h$ , are also plotted in Fig. 9. The largest  $\gamma_{cs,m}$ ,  $\gamma_{cs,s}$  and  $\gamma_{cs,v}$  of all STM models appear in that specified in EC 2. In particular, ACI 318-05 and EC 2 STMs are highly unconservative for deep beams without shear reinforcement. In addition, the unconservatism of both code models increases with the increase of  $h$ , regardless of the configuration of shear reinforcement, as shown in Fig. 9 (a) and (b). On the other hand,  $\gamma_{cs,m}$  of both code models decreases in deep beams with shear reinforcement compared with those without shear reinforcement, as both code models do not recommend a shear transfer mechanism of shear reinforcement. Predictions obtained from Tan and Cheng's model slightly overestimate the shear capacity of deep beams without shear reinforcement. Although, Tan and Cheng's model includes the size effect,  $\gamma_{cs}$  slightly decreases with the increase of  $h$  as shown in Fig. 9 (c). On the other hand, the predictions obtained from the present model are in better agreement with test results, regardless of the configuration of shear reinforcement, indicating that  $\gamma_{cs,m}$ ,  $\gamma_{cs,s}$  and  $\gamma_{cs,v}$  are 0.989, 0.245 and 0.248, respectively. In particular,  $\gamma_{cs}$  of the present model lies within a range of 0.6 to 1.8, regardless of the variation of  $h$  as shown in Fig. 9 (d).

## Parametric Study

The influence of longitudinal reinforcement ratio, web reinforcement and overall depth on the shear capacity of deep beams is evaluated using STMs of ACI 318-05, EC-2, Tang and Cheng and the current model. Experimental results are also extracted from the database and presented in the following figures, whenever possible, to validate the trend predicted by different models.

### Effect of longitudinal reinforcement ratio

The influence of longitudinal reinforcement ratio  $\rho_s$  on the normalized shear capacity,  $\lambda_n = V_n / (b_w h \sqrt{f'_c})$ , of deep beams is shown in Fig. 10. Geometrical dimensions, concrete strength and reinforcement details of deep beams considered are also presented in Fig. 10. It is generally accepted<sup>17, 23</sup> that  $\lambda_n$  increases with the increase of  $\rho_s$  up to a certain limit, dependent on  $a/h$ , beyond which  $\lambda_n$  remains constant. Predictions obtained from ACI 318-05 and EC 2 are not influenced by  $\rho_s$ , and different from each other. On the other hand, predictions obtained from Tan and Cheng's strut and tie model, and the present study increase with the increase of  $\rho_s$ . In particular, the increasing rate of  $\lambda_n$  predicted from the present model gradually descends with the increase of  $\rho_s$ , indicating that the effect of  $\rho_s$  incorporated in the present model is in good agreement with the general trend observed in the literature.

### Relative effectiveness of vertical and horizontal shear reinforcement

Fig. 11 shows the variation of  $\lambda_n = V_n / (b_w h \sqrt{f'_c})$  of deep beams with either vertical or horizontal shear reinforcement against the shear span to depth ratio  $a/h$ . Geometrical dimensions, concrete strength and reinforcement details of deep beams considered are also given in Fig. 11. The analytical results of ACI 318-05 and EC 2 are not presented in the figure, as they do not provide any guidelines for shear transfer mechanism of shear reinforcement. It is generally recognized<sup>16, 19, 20</sup> that the threshold of  $a/h$ , where both vertical and horizontal web reinforcements are equally



effective, is between 0.75 and 1.0. A higher  $\lambda_n$  exhibited by deep beams with only horizontal web reinforcement than beams with only vertical web reinforcement when  $a/h$  is less than this critical threshold. Predictions obtained from Tan and Cheng's model are seldom influenced by the configuration of shear reinforcement, though the threshold  $a/h$  appears at around 1.1. On the other hand, the effect of the vertical and horizontal shear reinforcements on  $\lambda_n$  changed against  $a/h$  is clearly demonstrated in the present model, showing that the threshold  $a/h$  is around 0.9. Therefore, the present model reasonably embodies the shear transfer mechanism of shear reinforcement by truss action. In addition, predictions from both STM models are reasonably close to experimental results of Yang et al.<sup>19</sup>.

### **Effect of overall depth of deep beams**

The influence of deep beam depth  $h$  on  $\lambda_n = V_n / (b_w h \sqrt{f'_c})$  carried out by Tan and Lu<sup>24</sup> is presented in Fig. 12. In all STMs and experimental results, it is clearly observed that  $\lambda_n$  decreases with the increase of  $h$ , but the decreasing rate varies. A higher decreasing rate is observed in predictions from the models of ACI 318-05, EC 2 or Tan and Cheng than in the present model. However, the decreasing rate of  $\lambda_n$  predicted from the present model is very close to that of test results, indicating that the size effect is properly reflected in the present model.

## **CONCLUSIONS**

A strut-and-tie (STM) model reflecting size effect based on the crack band theory of fracture mechanics is proposed to evaluate the shear transfer capacities of concrete struts and shear reinforcement in deep beams. The basic formulas for the shear transfer mechanism of concrete and shear reinforcement are driven using the energy equilibrium in the stress relief strip and crack band zone of concrete struts. Based on the statistical comparisons and parametric analysis presented, the following conclusions may be drawn:

1. The predictions obtained from the present model are in much better agreement with test results than those determined from STMs proposed by ACI 318-05 and EC 2. The mean, standard deviation, and coefficient of variation of the ratio between predicted using the present model and measured shear capacities are 1.002, 0.250 and 0.250, respectively.
2. The normalized shear capacity predicted from the present model increases with the increase of longitudinal reinforcement ratio and the increasing rate gradually descends with further increase of longitudinal reinforcement ratio, similar to trend generally observed in experimental results.
3. The effect of the vertical and horizontal shear reinforcements on the shear capacity of deep beams is reasonably reflected in the present model.
4. The normalized shear capacity of deep beams decreases with the increase of section overall depth, in particular, the decreasing rate predicted from the present model is in better agreement with test results than STM models of ACI 318-05, EC2 and Tan and Cheng.
5. The proposed model shows that the normalized shear capacity of deep beams is proportional to  $(h)^{-0.25}$ , where  $h$  indicates section overall depth.

### **ACKNOWLEDGMENTS**

This work was supported by the Grant of the Korean Ministry of Education, Science and Technology (The Regional Core Research Program/Bio-housing Research Institute).

### **REFERENCES**

1. MacGregor, J. G., and Wight, J. K., Reinforced Concrete: Mechanics and Design, Prentice Hall, Pearson Education South Asia Pte Ltd., 2006, 1111 pp.

2. Yang, K. H., and Ashour, A. F., "Code Modeling of Reinforced Concrete Deep Beam," Magazine of Concrete Research, V. 60, No. 6, 2008, pp. 441-454.
3. ACI Committee 318, "Building Code Requirements for Structural Concrete (ACI 318-05) and Commentary (318R-05)," American Concrete Institute (ACI), Farmington Hills, MI, 2005, 430 pp.
4. ACI Committee 318, "Building Code Requirements for Structural Concrete (ACI 318-99) and Commentary (318R-99)," American Concrete Institute (ACI), Farmington Hills, MI, 1999, 430 pp.
5. Schlaich, J., Schäfer, K., and Jennewein, M., "Toward a Consistent Design of Structural Concrete," Journal of the Prestressed Concrete Institute, V. 32, No. 3, 1987, pp. 74-150.
6. Schlaich, J., and Schäfer, K., "Design and Detailing of Structural Concrete Using Strut-and-Tie Models," The Structural Engineer, V. 69, No. 6, 1991, 13 pp.
7. Marti, P., "Basic Tools of Reinforced Concrete Beam Design," ACI Structural Journal, V. 82, No. 1, 1985, pp. 46-56.
8. Cook, W. D., and Mitchell, D., "Studies of Disturbed Regions near Discontinuities in Reinforced Concrete Members," ACI Structural Journal, V. 85, No. 2, 1988, pp. 206-216.
9. European Standard EN 1992-1-1:2004, Eurocode 2: design of concrete structures. British Standards Institution. 2004.
10. Comité Euro-International du Béton. CEP-FIP Model Code 1990 for Concrete Structures, Bulletin d'Information No. 213-214, *CEB-FIP 90*, Lausanne, 1993.
11. Ashour, A. F., and Yang, K. H., "Application of Plasticity Theory to Reinforced Concrete Deep Beams-A Review," Magazine of Concrete Research, V. 60, No. 9, 2008, pp. 657-664.
12. Foster, S. J., and Malik, A. R., "Evaluation of Efficiency Factor Models used in Strut-and-Tie Modelling of Nonflexural Members," Journal of Structural Engineering, ASCE, V. 128, No. 5, 2002, pp. 569-577.

13. Tan, K. H., and Cheng, G. H., "Size Effect on Shear Strength of Deep Beams: Investigating with Strut-and-Tie Model," *Journal of Structural Engineering*, ASCE, V. 132, No. 5, 2006, pp. 673-685.
14. Matamoros, A. B., and Wong, K. H., "Design of Simply Supported Deep Beams Using Strut-and-Tie Models," *ACI Structural Journal*, V. 100, No. 6, 2003, pp. 704-712.
15. Bažant, Z., P., and Planas, J., *Fracture and Size Effect in Concrete and Other Quasibrittle Materials*, CRC Press, New York, 1998, 616 pp.
16. Yang, K. H., Ashour, A. F., Song, J. K., and Lee, E. T., "Neural Network Modelling for Shear Strength of Reinforced Concrete Deep Beams," *Structures and Buildings*, V. 161, No. 1, 2008, pp. 29-39.
17. Yang, K. H., and Ashour, A. F., and Song, J. K., "Shear Capacity of Reinforced Concrete Beams Using Neural Network," *International Journal of Concrete Structures and Materials*, Korea Concrete Institute, V. 1, No. 1, 2008, pp. 63-73.
18. Bažant, Z., P., "Crack Band Model for Fracture of geomaterials," *Proceeding of 4<sup>th</sup> International Conference on Numerical Methods in Geomechanics*, V. 3, 1982, Z. Eisenstein, Ed., pp. 1137-1152.
19. Yang, K. H., Chung, H. S., and Ashour, A. F., "Influence of Section Depth on the Structural Behavior of Reinforced Concrete Continuous Deep Beams," *Magazine of Concrete Research*, V. 59, No. 8, 2007, pp. 575-586.
20. Yang, K. H., and Ashour, A. F., "Load Capacity of Reinforced Concrete Continuous Deep Beams," *Journal of Structural Engineering*, ASCE, V. 134, No. 6, 2008, pp. 919-929.
21. Tan, K. H., Kong, F. K., Teng, S., and Weng, L. W., "Effect of Web Reinforcement on High-Strength Concrete Deep Beams," *ACI Structural Journal*, V. 94, No. 5, 1997, pp. 572-582.
22. Bažant, Z., P., and Sun, H. H., "Size Effect in Diagonal Shear Failure: Influence of Aggregate Size and Stirrups," *ACI Materials Journal*, V. 84, No. 4, 1987, pp. 259-272.

23. Tan, K. H., Teng, S., Kong, F. K., and Lu, H. Y., "Main Tension Steel in High Strength Concrete Deep and Short Beams," *ACI Structural Journal*, V. 94, No. 6, 1997, pp. 752-768.
24. Tan, K. H., and Lu, H. Y., "Shear Behavior of Large Reinforced Concrete Deep Beams and Code Comparisons," *ACI Structural Journal*, V. 96, No. 5, 1999, pp. 836-845.

**Table 1-Statistical comparisons of predictions by different STM models and test results.**

Statistical values	Models	W/O	W/V	W/H	W/VH	Total
$\gamma_{cs,m}$	ACI 318-05	1.277	0.836	0.769	0.952	1.027
	EC 2	1.487	0.804	0.743	0.738	1.039
	Tan and Cheng	1.092	0.858	0.862	0.846	0.947
	This study	1.000	0.961	0.978	1.015	0.989
$\gamma_{cs,s}$	ACI 318-05	0.689	0.384	0.337	0.305	0.543
	EC 2	0.978	0.453	0.412	0.281	0.758
	Tan and Cheng	0.399	0.293	0.242	0.154	0.341
	This study	0.277	0.246	0.255	0.179	0.245
$\gamma_{cs,v}$	ACI 318-05	0.540	0.460	0.438	0.321	0.529
	EC 2	0.658	0.564	0.554	0.381	0.729
	Tan and Cheng	0.365	0.344	0.280	0.182	0.360
	This study	0.277	0.256	0.260	0.176	0.248

Note :  $\gamma_{cs,m}$ ,  $\gamma_{cs,s}$  and  $\gamma_{cs,v}$  indicate the mean, standard deviation, and coefficient of variation for the

factor  $\gamma_{cs} = (V_n)_{Pre.} / (V_n)_{Exp.}$ , respectively. W/O, W/V, W/H, and W/VH refer to deep beams without, with only vertical, with only horizontal and with orthogonal shear reinforcement, respectively.

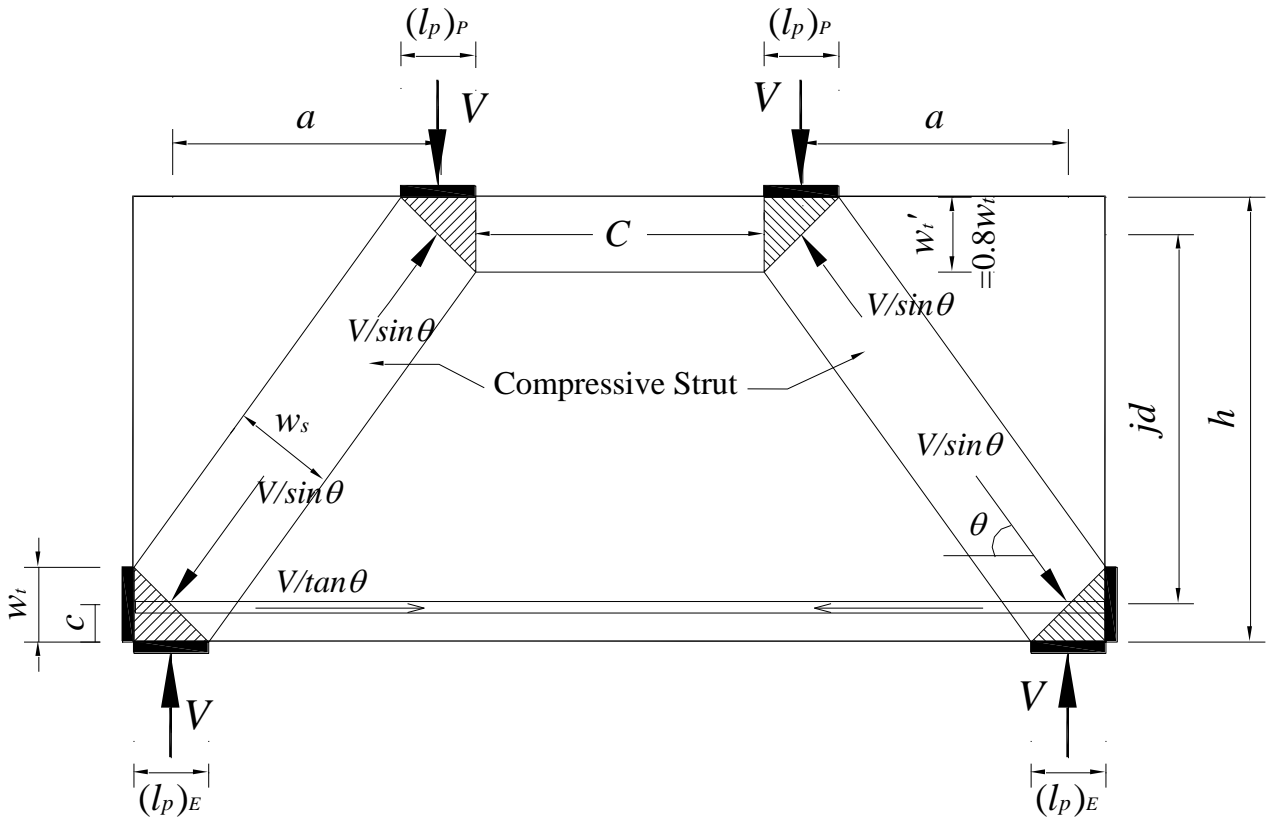


**Fig. 1– Schematic strut-and-tie model for simple deep beams.**

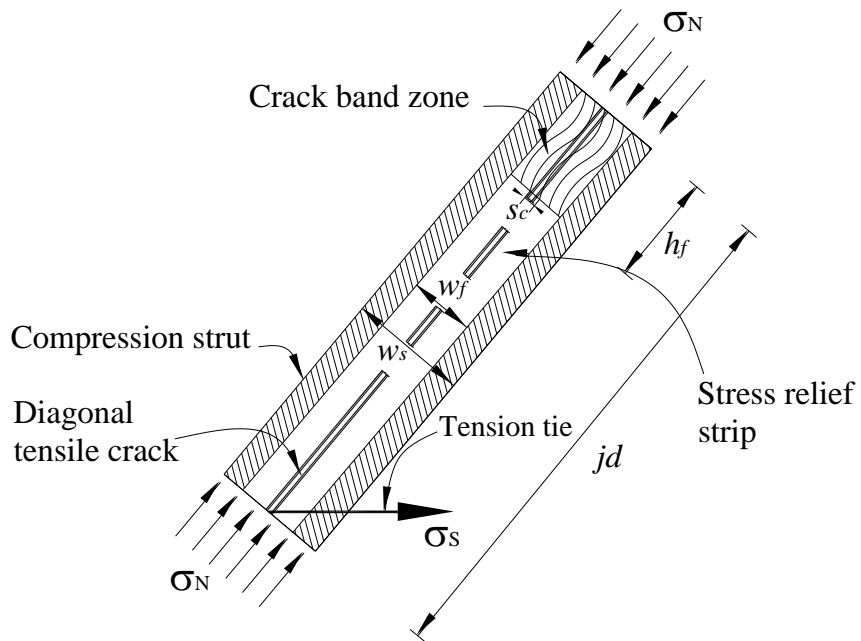


**Fig. 2- Idealized stress relief strip and crack band zone in beams without shear reinforcement.**

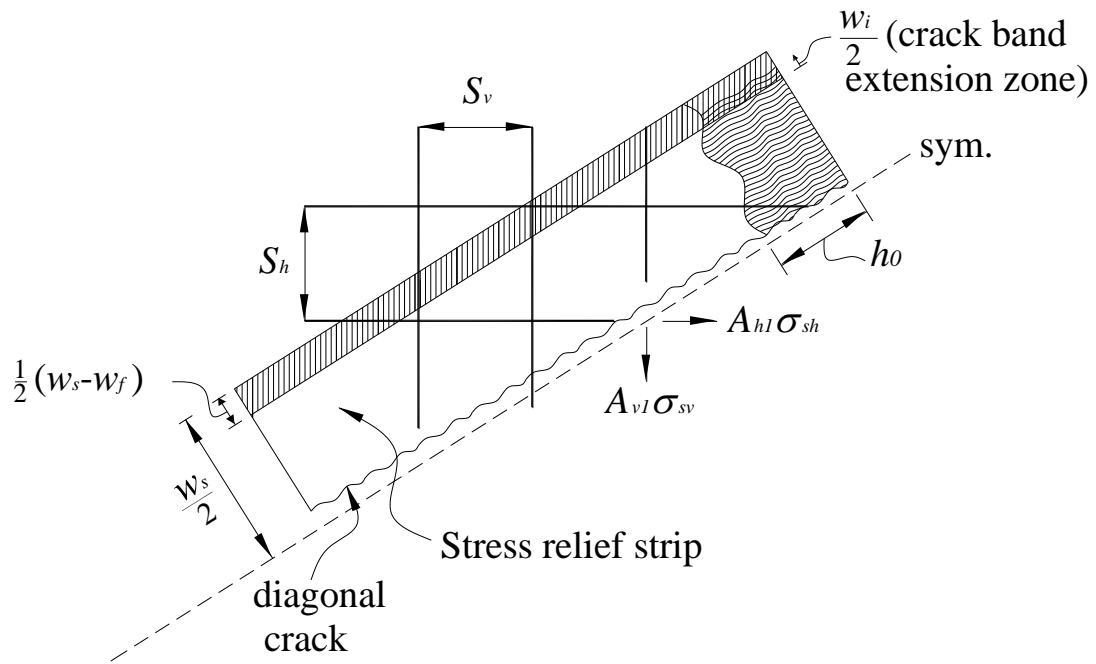


Fig. 3- Growth of crack band by shear reinforcement.

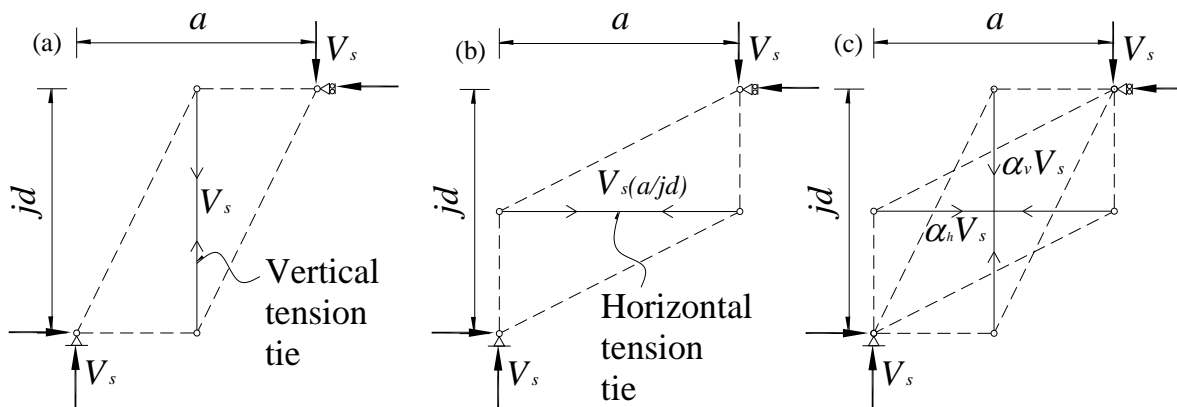
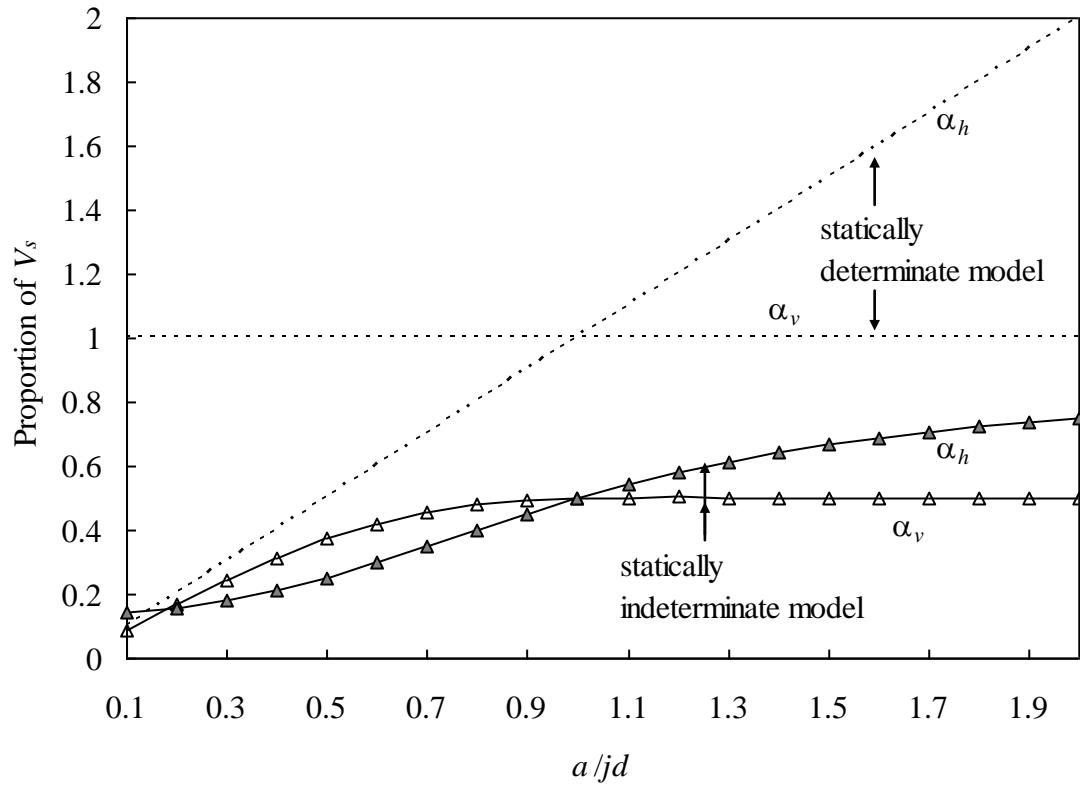
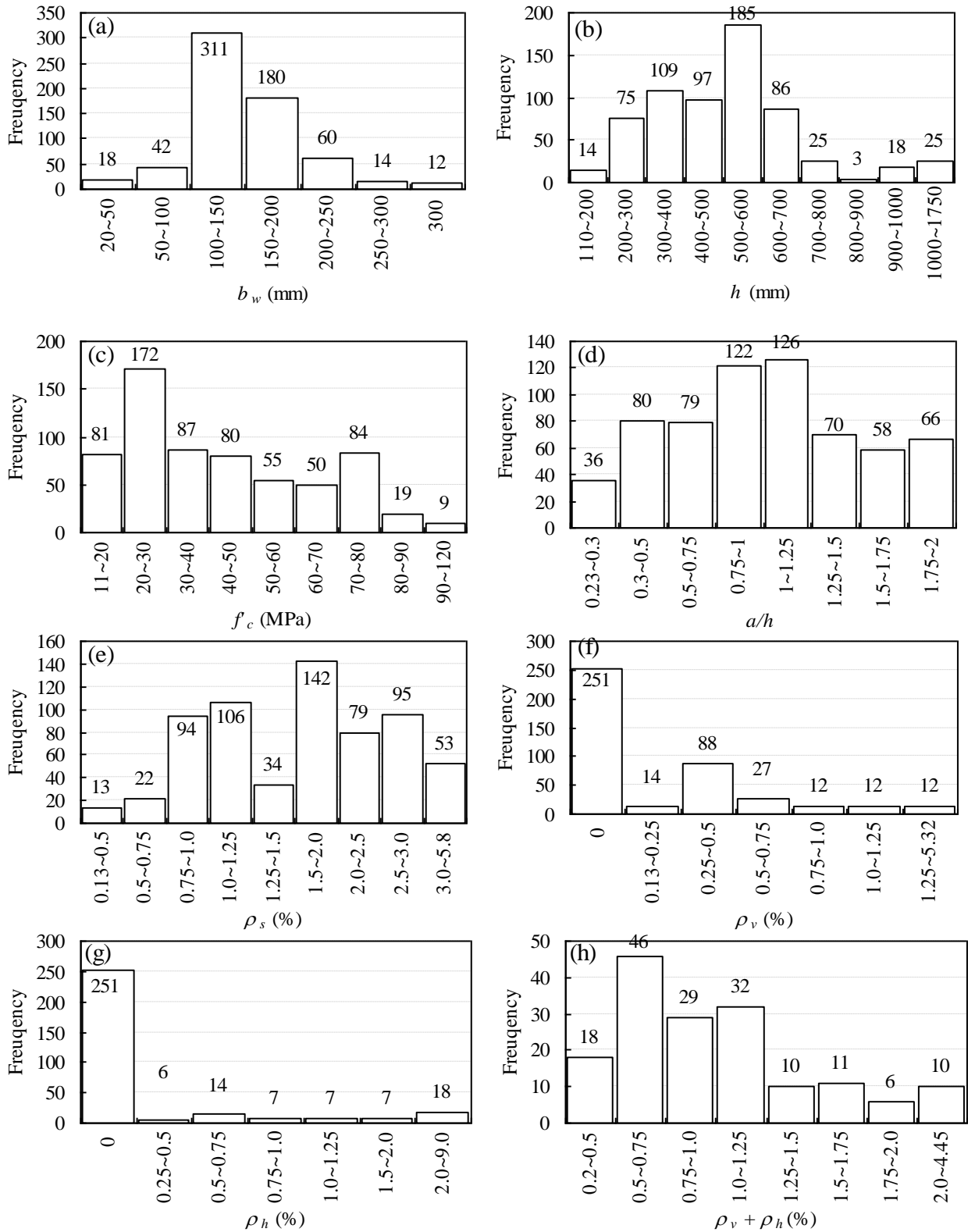


Fig. 4– Idealized shear transfer mechanism of shear reinforcement by truss action; (a) with vertical shear reinforcement only; (b) with horizontal shear reinforcement only; (c) with orthogonal shear reinforcement.





**Fig. 5– Proportion of shear force carried by horizontal and vertical shear reinforcement.**



**Fig. 6–Frequency distribution of main parameters in the database; (a) beam width; (b) beam overall depth; (c) concrete strength; (d) shear span-to-overall depth ratio; (e) longitudinal tensile reinforcement ratio; (f) vertical shear reinforcement ratio; (g) horizontal shear reinforcement ratio; (h) orthogonal shear reinforcement ratio.**

(1 MPa = 145 psi; 1 mm = 0.039 in.)

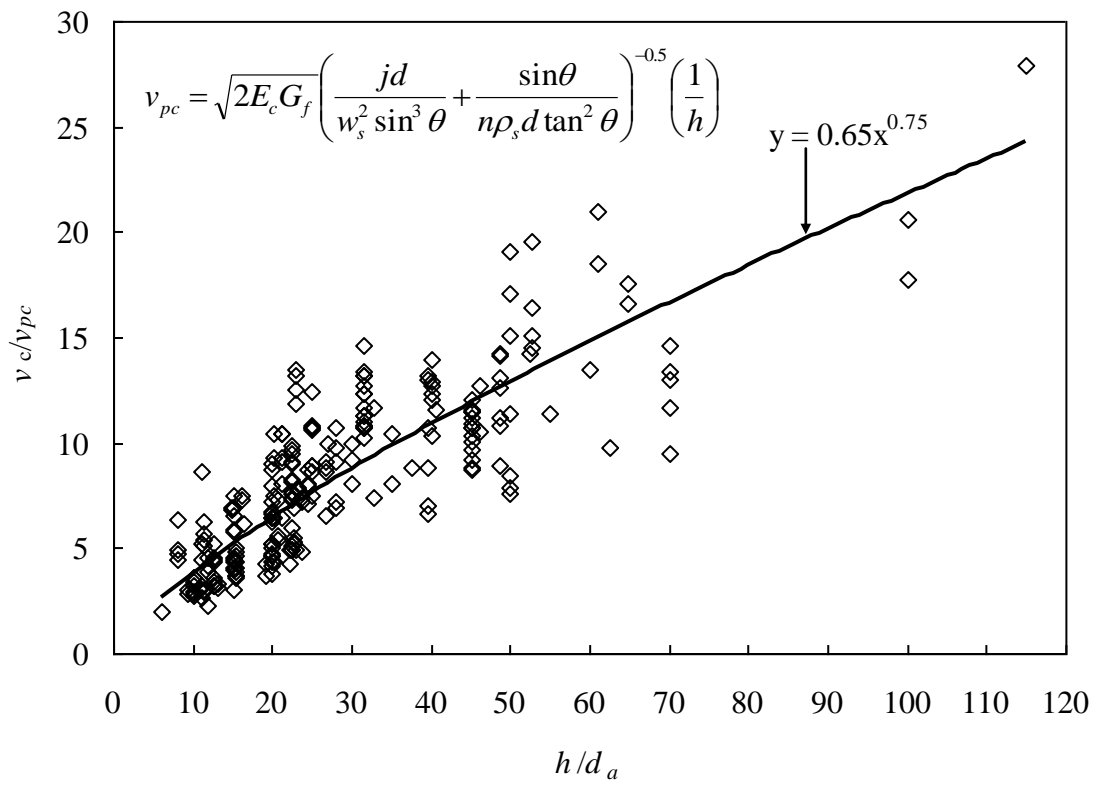


**Fig. 7– Normalized shear transfer capacity of deep beams without shear reinforcement.**

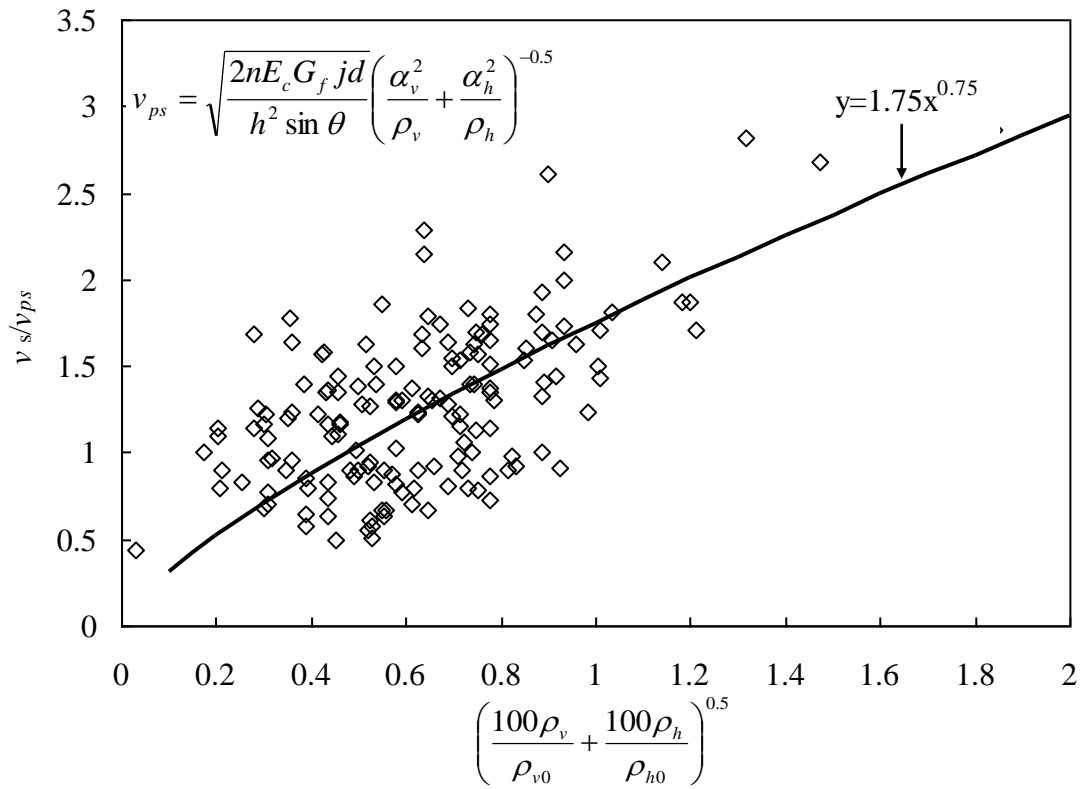
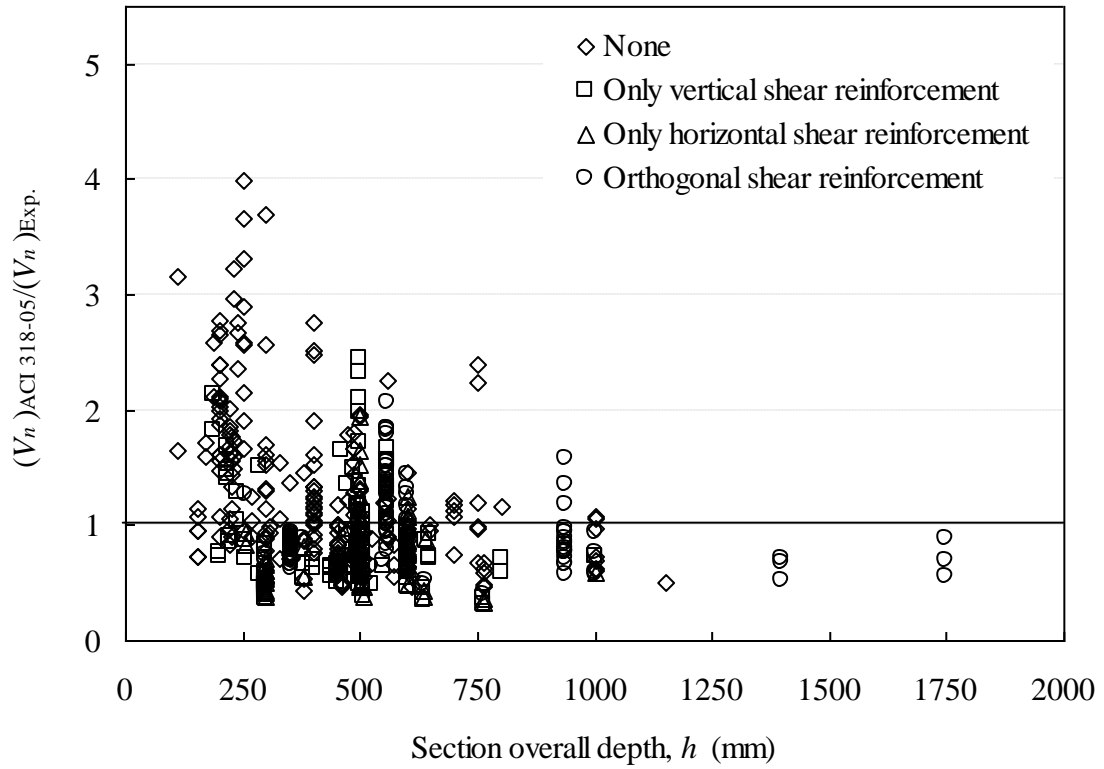
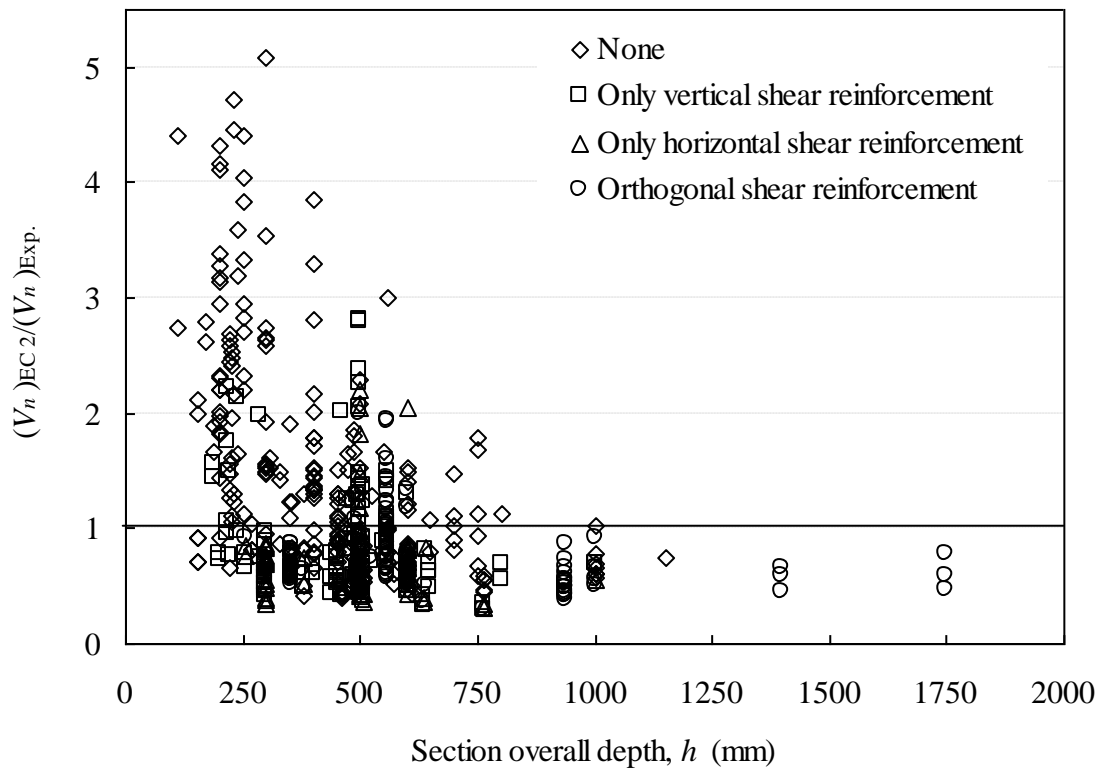


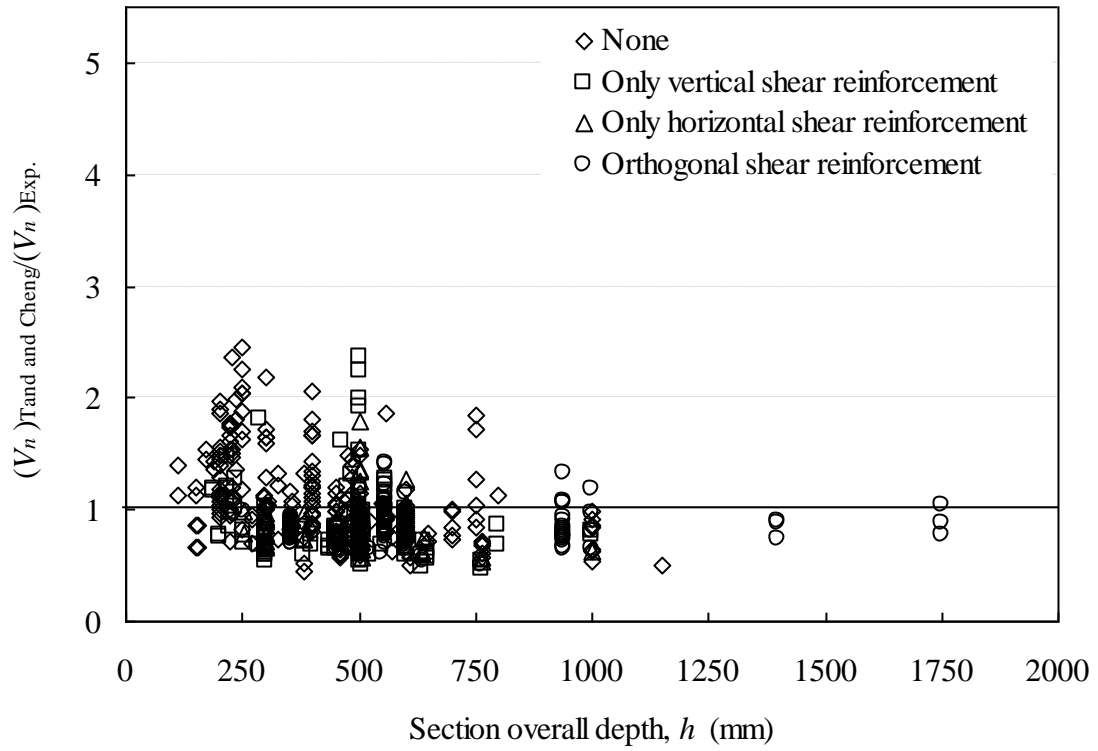
**Fig. 8– Normalized shear transfer capacity of shear reinforcement by truss action.**



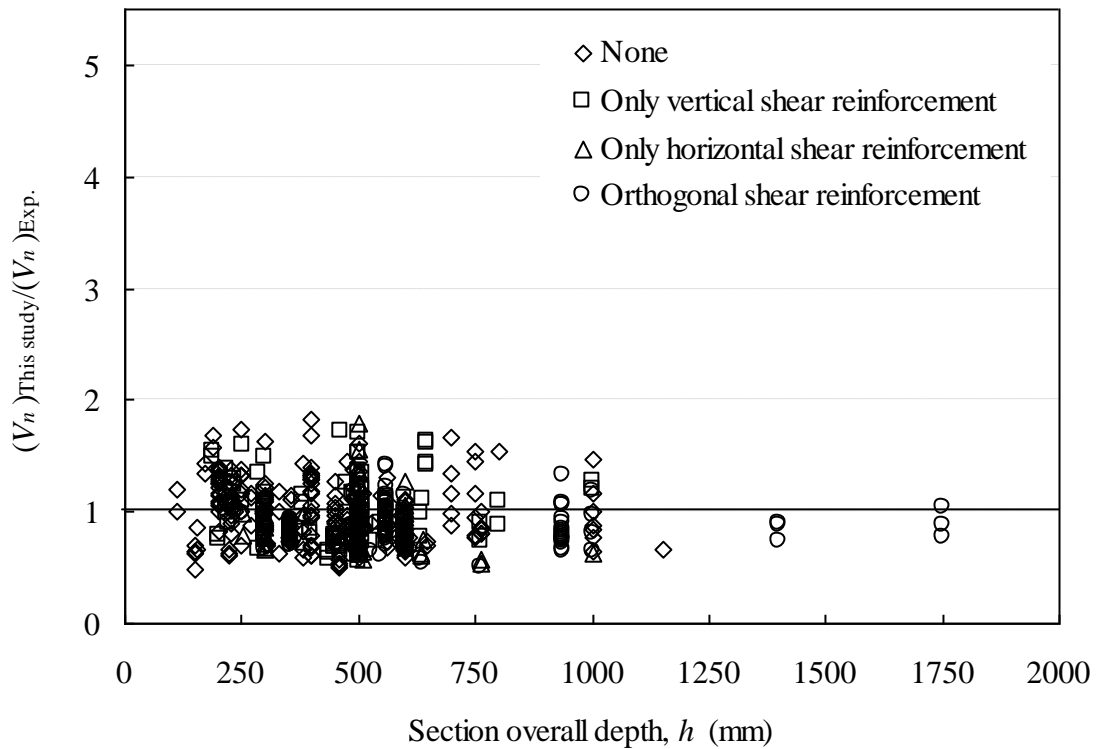
(a) ACI 318-05



(b) EC 2



(c) Tan and Cheng



(d) This study

**Fig. 9-Comparisons of predicted and measured shear capacities.**

(1 mm = 0.039 in.)

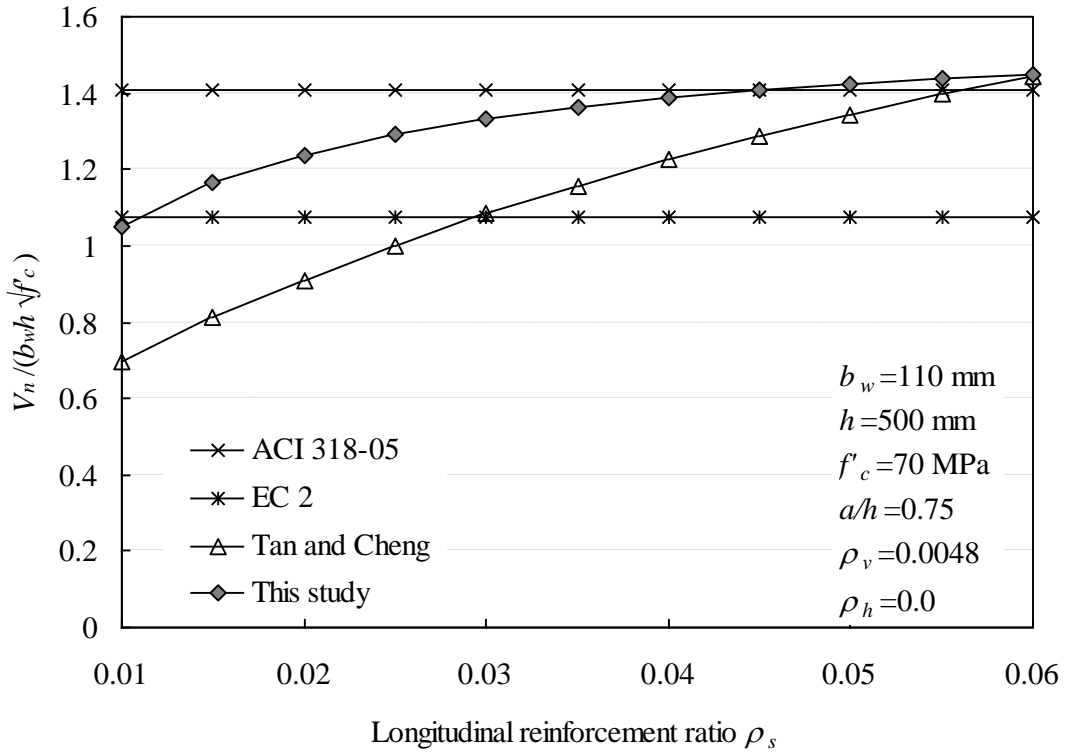


**Fig. 10 – Effect of  $\rho_s$  on normalized shear capacity of deep beams with  $a/h=0.75$ .**  
 (1 MPa = 145 psi; 1 mm = 0.039 in.)

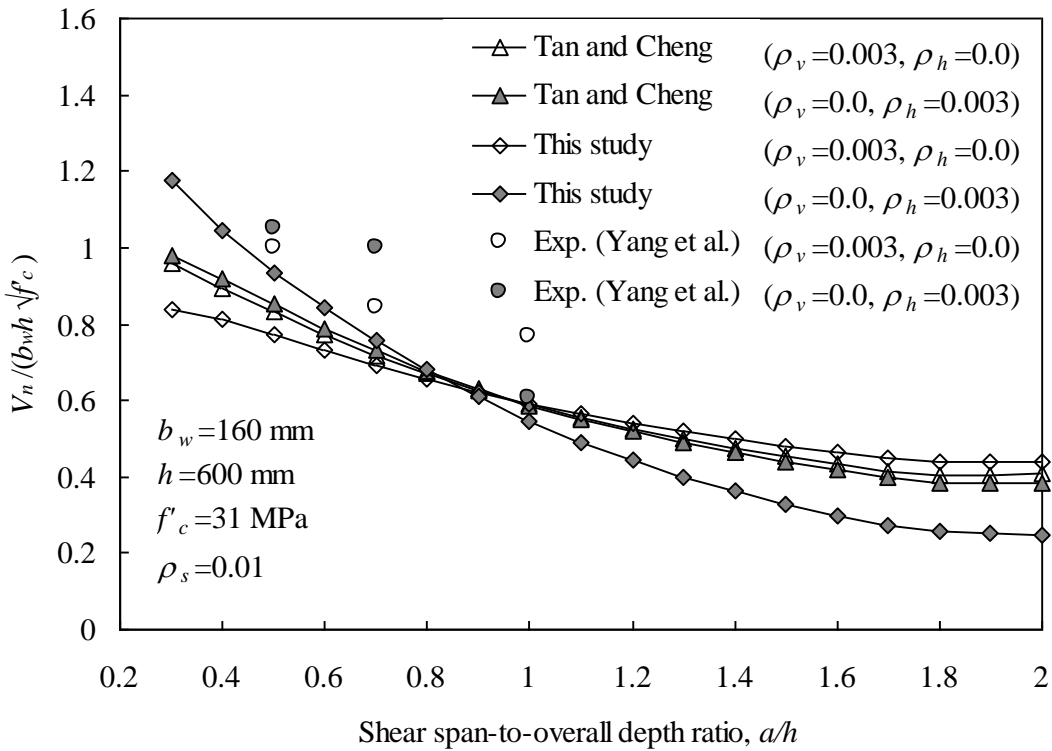


**Fig. 11 – Relative effectiveness of vertical and horizontal shear reinforcement against  $a/h$ .**

(1 MPa = 145 psi; 1 mm = 0.039 in.)

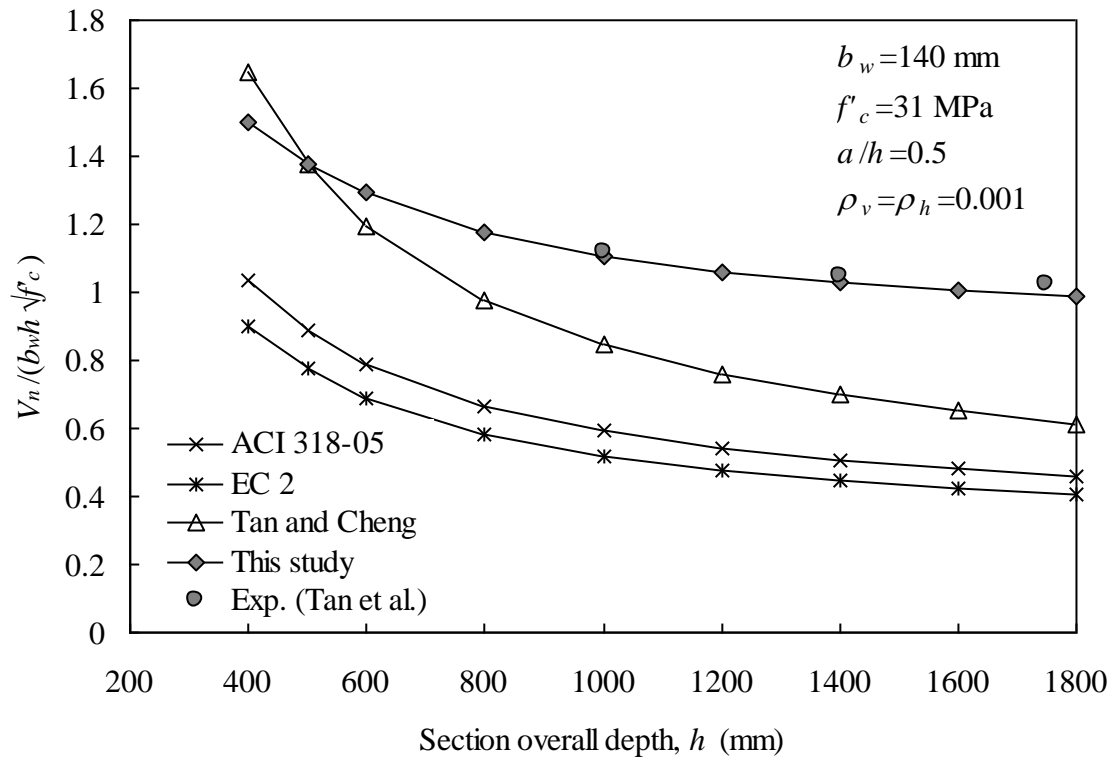


**Fig. 12 – Effect of  $h$  on normalized shear capacity of deep beams.**

(1 MPa = 145 psi; 1 mm = 0.039 in.)